REACTIVE ADSORPTION OF AMMONIA ON MODIFIED ACTIVATED CARBONS

Camille Petit, Ecole Nationale Superieure de Chimie de Montpellier, 8 rue de l'Ecole Normale, 34296 Montpellier, France.
Teresa J. Bandosz, Department of Chemistry, The City College of New York, The Graduate School of the City University of New York, 138 St. Convent Ave, New York, NY 10031, USA.
Email: tbandosz@ccmy.cuny.edu

Introduction

Current environmental concerns focus on a growing contamination caused by the release of chemicals, as for instance ammonia. Indeed, this industrial gas demonstrates toxic effects on human body (Issley, 2007) and causes also air pollution via its oxidation to nitric oxides (Manahan, 1999).

This has motivated research activities in the field of ammonia removal via adsorption process. Several sorbents such as zeolites, alumina and activated carbons have shown promising properties (Helminen et al., 2001; Sharanov et al., 2005; Domingo-García et al., 2002; Mangun et al., 1999; Park and Kim, 2005; Yin et al., 1999; Ellison et al., 2004; Valyon et al., 1998; Bandosz and Le Leuch, 2007; Stoeckli et al., 2004; Guo et al., 2005; Mangun et al., 1999; Le Leuch et al., 2005).

Yet, despite their encouraging adsorption efficiency in ammonia removal, activated carbons still do not provide specific and strong interactions (acid/base interactions, complexation, precipitation…) with the gas studied. To develop those stronger interactions, some researchers have modified activated carbon via oxidation (Bandosz and Le Leuch et al., 2007; Guo et al., 2005; Mangun et al., 1999), impregnation with metal oxides (Stoeckli et al., 2004), or metal chlorides (Sharanov et al., 2005).

Besides the involvement of specific forces between ammonia and the adsorbent, it has been demonstrated that the presence of water could also improve ammonia removal (Bandosz and Le Leuch, 2007) by forming ammonium ions that interact with carbon's acidic groups.

In the present work, the ammonia removal by activated carbons impregnated with different metal chlorides ($ZnCl_2$, $NiCl_2$ and $CuCl_2$) has been investigated for various moisture contents. The goal was to test the influence of several experimental parameters such as the type of metal, the metal loading, or the presence of water in the system.

Experimental

Materials

BPL carbon (Calgon Corporation) was impregnated with either zinc, nickel or copper chlorides. In the latter case, two different amounts of metal chlorides were used. The composition of the four resulting activated carbons is given in Table 1.

Table1. Content of the carbon samples after impregnation with metal chlorides.

Sample	C-$ZnCl_2$	C-$NiCl_2$	C-$CuCl_2$A	C-$CuCl_2$B
Salt added to the virgin carbon	$ZnCl_2$	$NiCl_2.6H_2O$	$CuCl_2.2H_2O$	$CuCl_2.2H_2O$
Percentage of metal chloride (wt%)	20.4	16.9	19.2	10.9
Percentage of metal (wt%)	9.81	7.67	9.08	5.17
Percentage of metal (mmol/g)	1.50	1.31	1.43	0.813

Ammonia breakthrough capacity

The efficiency of the previously impregnated carbons was tested for the ammonia removal in dynamic conditions: a flow of ammonia (concentration: 1000ppm) diluted in air (total flow rate: 900ml/min) went through a fixed bed of a carbon sample. The adsorbent's bed contained granules of carbons with a size between 1 and 2 mm packed into a glass column. The size of bed was 80 mm x 10 mm. To evaluate the influence of water, each sample was exposed to either ammonia diluted in dry air (C-MCl_2-ED, M referring

to the metal and ED to "Dry air"), or ammonia diluted in moist air (C-MCl$_2$-EM, EM referring to "Moist air"). Those two experiments were repeated after a 2-hour prehumidification step (C-MCl$_2$-EPD and C-MCl$_2$-EPM respectively, P standing for prehumidification).

Analyses
The different samples (virgin and impregnated carbons) were characterized before and after exposure to ammonia, using sorption of nitrogen, thermal and XRF analysis, XRD, SEM and FTIR.

Results and discussion

Adsorption capacity along with ammonia breakthrough curves for all samples (virgin and impregnated carbons) are collected in Table 2 and Figure 1, respectively.

From this table, one can see that the adsorption capacity is dramatically improved after impregnation with metal chlorides: almost two orders of magnitude are reached compared to the initial BPL carbon. The best results are obtained for C-CuCl$_2$A and C-NiCl$_2$.

Table 2. NH$_3$ breakthrough capacity, amount of adsorbed water, and surface pH.

Sample	NH$_3$ breakthrough capacity (mg/g of carbon)	Water adsorbed (mg/g)	pH initial	pH final
C-ED	0.8	-	7.87	7.92
C-EM	0.9	-	7.87	7.44
C-EPD	2.2	236	7.87	7.51
C-EPM	2.0	245	7.87	7.41
C-ZnCl$_2$-ED	51.7	-	6.15	7.10
C-ZnCl$_2$-EM	58.4	-	6.15	7.28
C-ZnCl$_2$-EPD	55.3	246	6.15	6.99
C-ZnCl$_2$-EPM	65.0	247	6.15	7.97
C-NiCl$_2$-ED	58.9	-	6.98	8.60
C-NiCl$_2$-EM	80.8	-	6.98	8.48
C-NiCl$_2$-EPD	59.2	286	6.98	8.50
C-NiCl$_2$-EPM	73.9	273	6.98	8.65
C-CuCl$_2$A-ED	67.7	-	4.19	9.04
C-CuCl$_2$A-EM	62.8	-	4.19	8.56
C-CuCl$_2$A-EPD	62.7	256	4.19	8.72
C-CuCl$_2$A-EPM	70.6	231	4.19	8.84
C-CuCl$_2$B-ED	29.1	-	4.69	8.47
C-CuCl$_2$B-EM	38.7	-	4.69	8.64
C-CuCl$_2$B-EPD	33.7	269	4.69	8.63
C-CuCl$_2$B-EPM	34.2	286	4.69	8.41

For all samples but C-CuCl$_2$A, the adsorption capacity follows that trend: ED < EM and EPD < EPM. This means that water enhances the adsorption efficiency as observed previously (Bandosz and Le Leuch, 2007). It is also interesting to notice that C-CuCl$_2$B demonstrates an adsorption capacity that is almost twice lower than the adsorption capacity of C-CuCl$_2$A. This can be directly linked to the metal chloride loading of those carbons: 19.2 wt% for C-CuCl$_2$A and 10.9 wt% for C-CuCl$_2$B. The breakthrough capacity curves show a similar vertical shape for all samples (virgin and impregnated carbons) indicating fast interactions of ammonia with adsorbents' surface.

Changes in the carbon bed's color were observed during ammonia adsorption. In the case of zinc-containing samples, some white spots appeared whereas some adsorbents' particles became "blue-green" during the experiments run on C-CuCl$_2$A. Those changes are related to a reactive adsorption on solids' surface. They must be due to the formation of salts involving ammonia and metal chlorides deposited on the carbon surface. In the case of C-NiCl$_2$ and C-CuCl$_2$B, we did not observe any change, probably because salts are too dispersed to be detected. The nature of those solids will be discussed more deeply with X-Ray analyses and DTG curves.
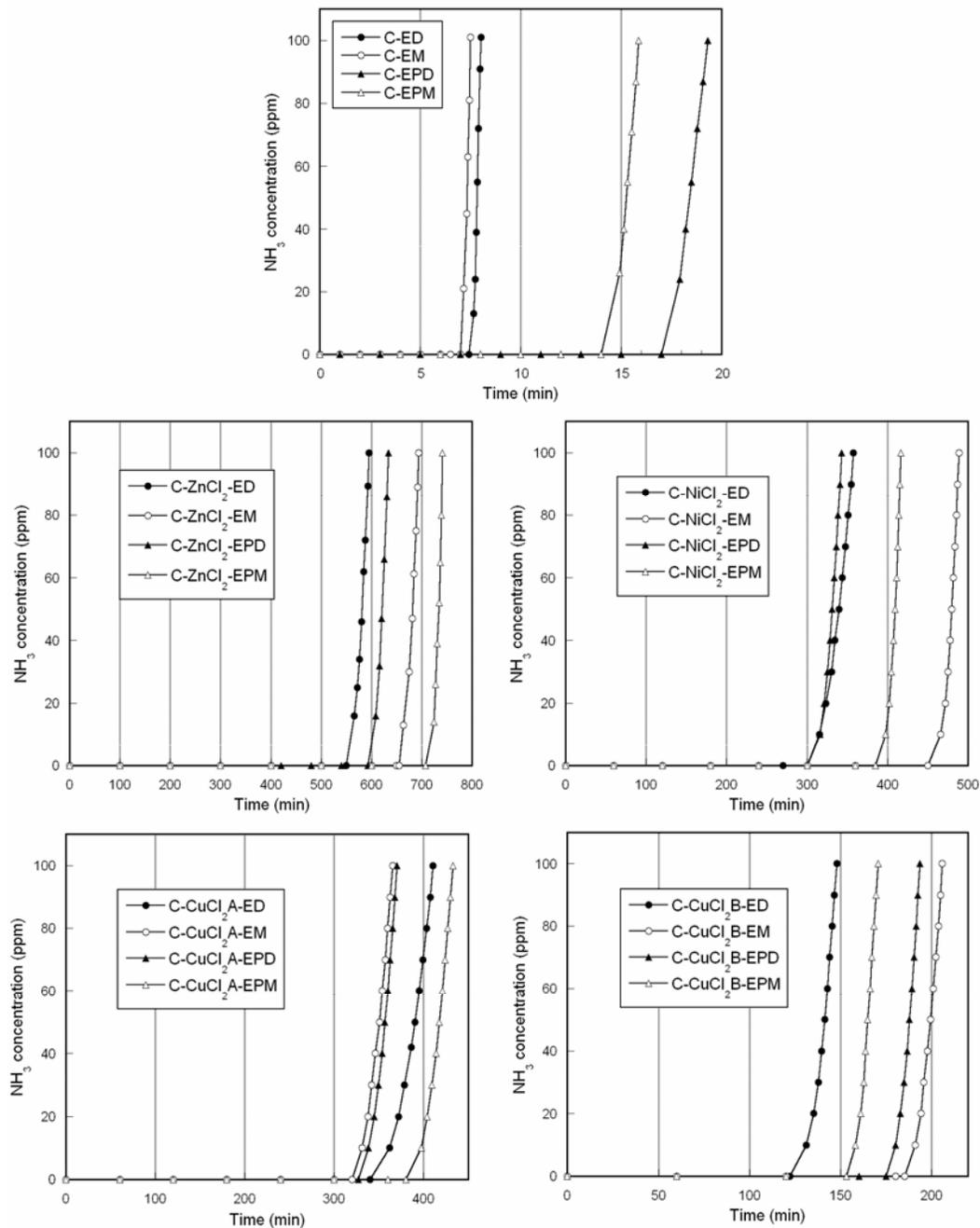
**Figure 1.** Ammonia breakthrough curves for the initial and impregnated carbons.

To understand the improvement in the adsorbent's efficiency after impregnation with metal chlorides, it can be useful to consider the structural parameters of the different samples before and after exposure to ammonia (Table 3). The PSDs curves are collected in (Figure 2). At first, we can notice a decrease in all structural parameters after impregnation as a consequence of metal chloride deposition over the carbon surface.

As seen from Figure 2, an additional microporosity is formed after ammonia adsorption for C-NiCl$_2$ and C-CuCl$_2$A samples. This can be linked to the formation of salts between ammonia and metal chloride species. Those new solids should be deposited in larger pores and thus contribute to the formation of a

secondary porosity. On the contrary, for C-ZnCl$_2$ and C-CuCl$_2$B samples, a decrease in the pore volume is observed after ammonia adsorption. These different trends between the impregnated carbons suggest that the location and the dispersion of metal chlorides are an important factors affecting sorbent's efficiency.

Table 3. Structural parameters calculated from nitrogen adsorption isotherms for the initial carbons.

Sample	S_{BET} (m^2/g)	V_t (cm^3/g)	V_{meso} (cm^3/g)	V_{mic} (cm^3/g)	V_{mic}/V_t
C	1033	0.614	0.139	0.475	0.774
C-ZnCl$_2$	726	0.437	0.095	0.342	0.783
C-NiCl$_2$	646	0.395	0.096	0.299	0.757
C-CuCl$_2$A	565	0.345	0.095	0.250	0.725
C-CuCl$_2$B	914	0.539	0.124	0.415	0.770
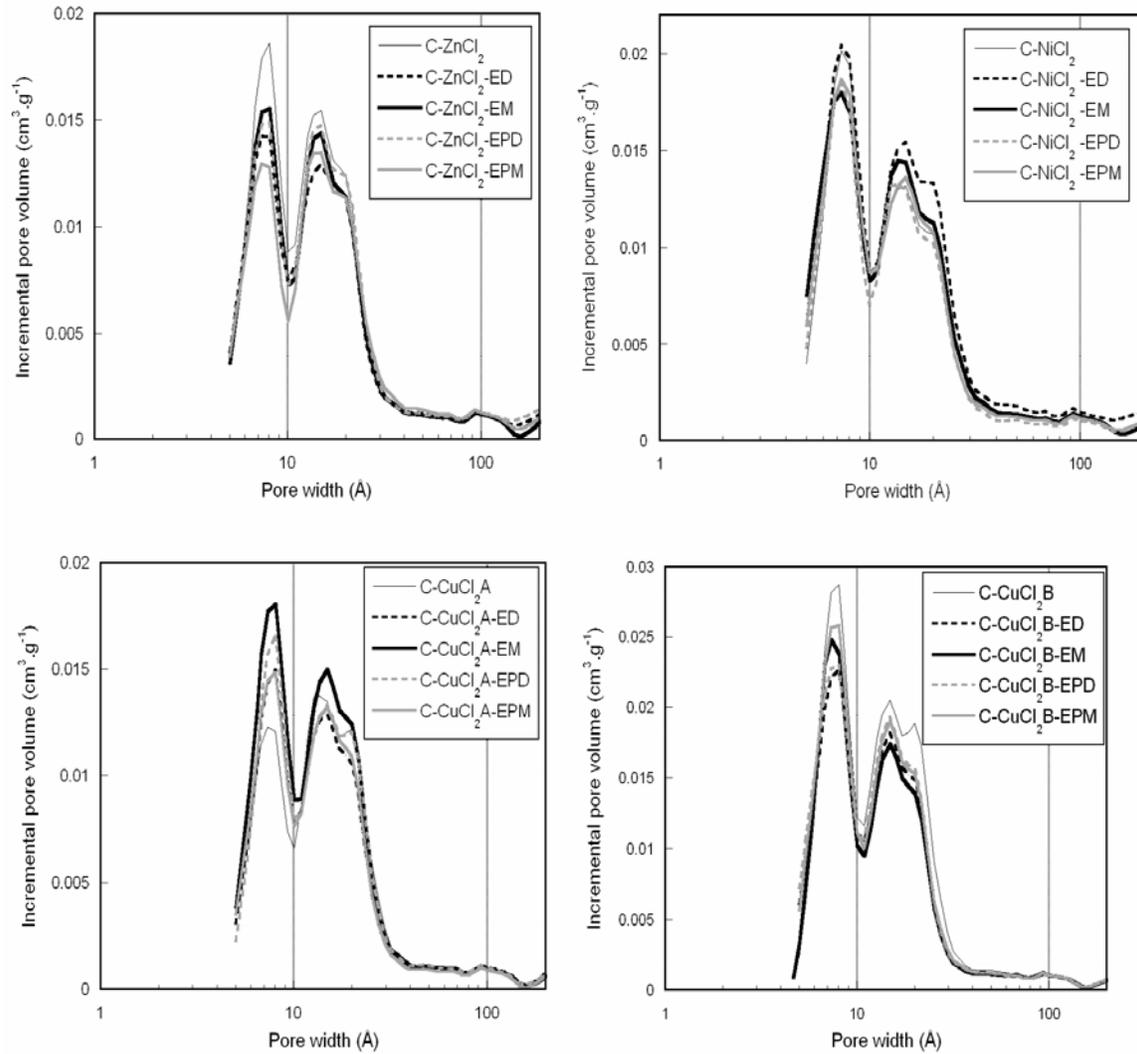
Figure 2. Pore size distribution for the impregnated carbons after NH$_3$ adsorption.

X-Ray diffraction patterns reported in Figure 3 provide some interesting insight of the nature and the dispersion of the metal chlorides and the salts involved in our study. It should be reminded that the sharper

and better defined peaks are, the less dispersed is the compound. For the initial impregnated samples, no well defined peaks are detected indicating a good dispersion of metal chloride over carbon's surface.
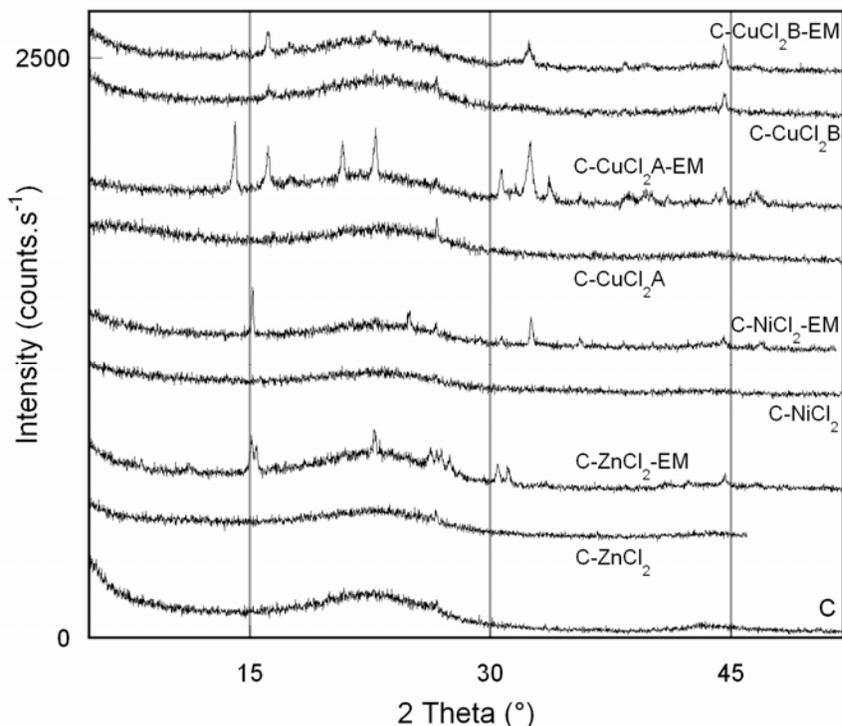
Figure 3. XRD spectra for the initial and impregnated carbons before and after NH_3 adsorption.

Considering the exhausted samples, one can observe the apparition of new peaks. In the case of C-$ZnCl_2$, peaks at 2Theta 15.1, 27.5 and 15.5, 31.2 can be attributed to the presence of $ZnCl_2$ and $ZnCl_2 2NH_4Cl$ respectively. For C-$CuCl_2$A, $CuCl_2 2NH_4Cl_2H_2O$ is detected at 2Theta 16.1, 32.5 and 33.9. For the nickel-containing exhausted sample, only $NiCl_2 6H_2O$ is clearly seen at 2Theta 15.2 and 25.0, which suggests that the ammonium complexes with nickel are well dispersed on the carbon surface.

The nature of those complexes was also identified via DTG curves as seen in Figure 4. A first peak between 50 and 130^{0}C related to the removal of physically adsorbed water is detected for the initial impregnated samples. Another broad peak at 500^{0}C indicates the presence of metal chloride. After exposure to ammonia, an additional broad peak appears between 130 and 400^{0}C for zinc and nickel-containing samples. In the former case, this peak represents ammonium tetrachlorozincate (Weast, 1986). For C-$NiCl_2$, no certitude on the nature of this peak could be reached. It could be attributed to either $NiCl_2 6H_2O$ (Charles et al., 2001) or ammonium nickel chloride (Weast, 1986; Kirby, 1961).

For the samples impregnated with copper, two peaks are observed in the ranges 130-210^{0}C and 210-310^{0}C. They must be related to the presence of ammonium copper chloride and copper diammine chloride (Weast, 1986) respectively. This latter complex was previously encountered in ammonia adsorption onto Cu-ZSM zeolites (Valyon et al., 1998).

Ammonia detected in DTG curves can be considered as strongly adsorbed ammonia since it does not desorb before 200^{0}C. Consequently, DTG curves were used to calculate the amount of strongly adsorbed ammonia. The results are given in Table 4.

As seen from this table, the amount of weakly adsorbed ammonia is significantly higher than the amount of strongly adsorbed ammonia indicating that most of the ammonia is adsorbed via non-specific interactions such as hydrogen bonding or Van der Waals interactions. C-$CuCl_2$A sample has the best ratio NH_3 breakthrough capacity and NH_3 strongly adsorbed. Thus its surface must be the most inclined to form strong specific interactions with ammonia. Even though C-$CuCl_2$B sample contains less metal chloride than

C-ZnCl$_2$ sample, the amount of strongly adsorbed ammonia remains similar in those two cases. This is related to the metal dispersion on the carbon surface.
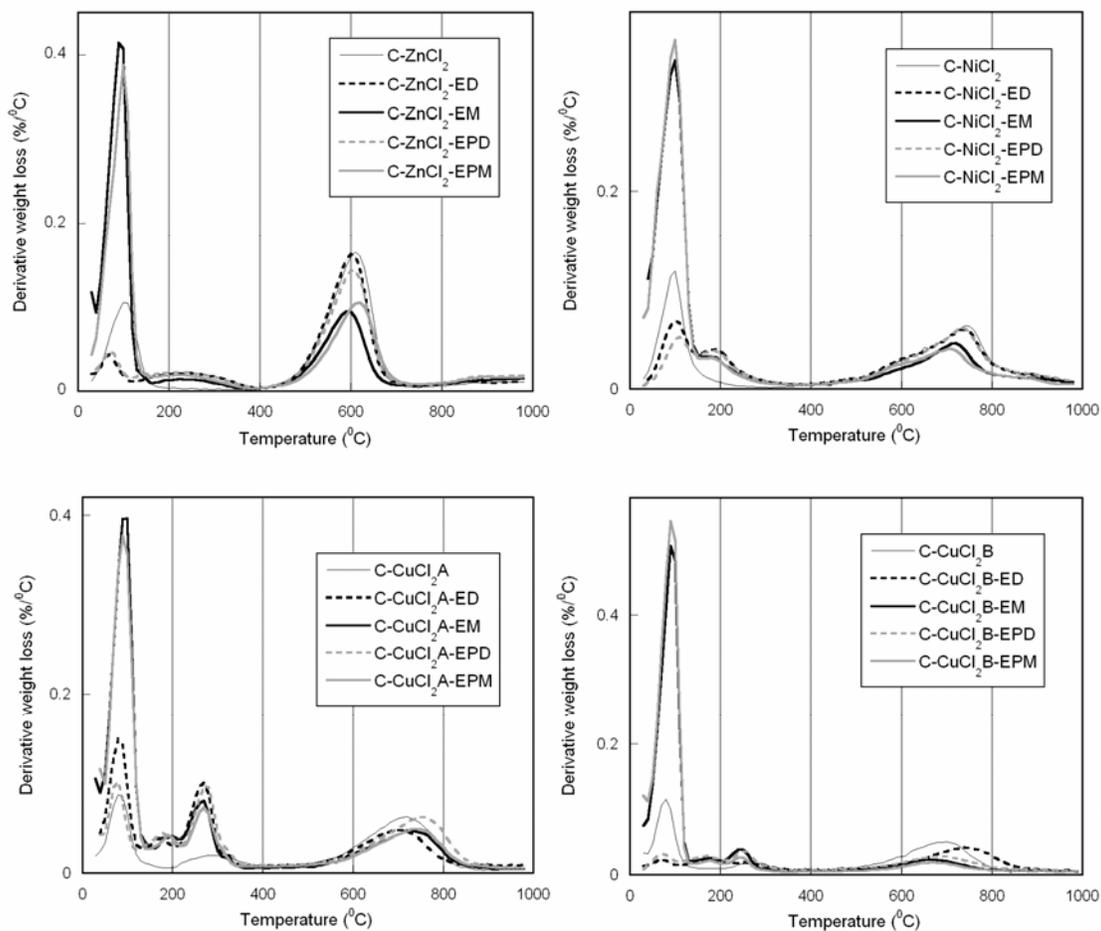
Figure 4. DTG curves of the impregnated samples before and after NH$_3$ adsorption.

Table 4. Amount of weakly and strongly adsorbed ammonia.

Sample	Amount of weakly adsorbed NH$_3$		Amount of strongly adsorbed NH$_3$	
	(mg/g of carbon)	(mmol/mol of metal)	(mg/g of carbon)	(mmol/mol of metal)
C-ZnCl$_2$-ED	45.5	1784	6.2	243
C-ZnCl$_2$-EM	54.1	2122	4.3	169
C-ZnCl$_2$-EPD	47.5	1863	7.8	306
C-ZnCl$_2$-EPM	60.2	2361	4.8	188
C-CuCl$_2$A-ED	51.6	2123	16.1	662
C-CuCl$_2$A-EM	48.5	1995	14.3	588
C-CuCl$_2$A-EPD	46.8	1925	15.9	654
C-CuCl$_2$A-EPM	57.6	2369	13.0	535
C-CuCl$_2$B-ED	24.5	1773	4.6	333
C-CuCl$_2$B-EM	31.8	2301	6.9	499
C-CuCl$_2$B-EPD	26.7	1932	7.0	506
C-CuCl$_2$B-EPM	29.3	2120	4.9	355

Conclusion

The present study underlines the important role of metal chlorides for ammonia adsorption. A significant increase in adsorption capacity was reached after impregnation of BPL carbon with $ZnCl_2$, $NiCl_2$ or $CuCl_2$, with the best results obtained for the copper-containing carbon. Metal chlorides enable a reactive adsorption of ammonia on the activated carbon surface via the formation of complexes. Yet, those specific interactions are not predominant and most of the ammonia is weakly adsorbed. It has also been demonstrated that the metal dispersion and the presence of water are important parameters that determine ammonia adsorption.

Acknowledgments

References

Bandosz, T. J.; Le Leuch, L. M. 2007. The role of water and surface acidity on the reactive adsorption of ammonia on modified activated carbons. *Carbon* 45(3):568-578.

Charles, J.N.; Deshpande, N.D.; Deshpande, D.A. 2001. Dehydratation of $NiCl_2 6H_2O$. *Thermochimica Acta* 375:169-176.

Domingo-García, M.; Groszek, A. J.; López-Garzón, F. J.; Perez-Mendoza, M. 2002. Dynamic adsorption of ammonia on activated carbons measured by flow microcalorimetry. *Applied Catalysis A: General* 233:141-150.

Ellison, M. D.; Crotty, M. J.; Koh, D. K.; Spray, R. L; Tate, K. E. 2004. Adsorption of NH_3 and NO_2 on Single-Walled Carbon Nanotubes. *J. Phys. Chem. B* 108(23):7938-7943.

Guo, J.; Xu, W. S.; Chen, Y. L.; Lua, A. C. 2005. Adsorption of NH_3 onto activated carbon prepared from palm shells impregnated with H_2SO_4. *J. Colloid Interf. Sci.* 281(2):285-290.

Helminen, J.; Helenius, J.; Paatero, E. 2001 Adsorption Equilibria of Ammonia Gas on Inorganic and Organic Sorbents at 298.15 K. *J. Chem. Eng.* 46(2):391-399.

Issley, S. 2007. Toxicity, ammonia. *Medline*. www.emedicine.com/EMERG/topic846.htm

Kirby, L. J. 1961. The radiochemistry of nickel. *National Academy of Sciences*, Washington D. C:3-13

Le Leuch, L. M.; Subrenat, A.; Le Cloirec, P. 2005. Hydrogen Sulfide and Ammonia Removal on Activated Carbon Fiber Cloth-Supported Metal Oxides. *Environmental Technology* 26:1243-1254.

Mangun, C. L.; Benak, K. R.; Daley, M. A.; Economy, J. 1999. Oxidation of Activated Carbon Fibers: Effect on Pore Size, Surface Chemistry, and Adsorption *Properties. Chem. Mater.* 11(12):3476-3483.

Mangun, C. L.; Braatz, R.D.; Economy, J.; Hall, A. J. 1999. Fixed Bed Adsorption of Acetone and Ammonia onto Oxidized Activated Carbon Fibers. *Ind. Eng. Chem. Res.* 38(9):3499-3504.

Manahan, S. E. 1999. *Environmental Chemistry 7th Edition*. Lewis, Boca Raton

Park, S-J.; Kim, B-J. 2005. Ammonia removal of activated carbon fibers produced by oxyfluorination. *J. Colloid Interf. Sci.* 291(2):597-599.

Stoeckli, F.; Guillot, A.; Slasli, A. M.; 2004. Specific and non-specific interactions between ammonia and activated carbons. *Carbon* 42:1619-1624.

Valyon, J.; Onytestyak, G.; Rees, L. V. C. 1998. Study of the dynamics of NH_3 adsorption in ZSM-5 zeolites and the acidity of the sorption sites using the frequency-response technique. *J. Phys. Chem. B* 102(45):8994-9001.

Weast, R. C. 1986. *Handbook of Chemistry and Physics 67th Ed*. R.C. West Ed.; Academic Press, Boca Raton, FL.

Yin, X.; Han, H.; Gunji, I.; Endou, A.; Ammal, S. S. C.; Kubo, M.; Miyamoto, A. 2004. NH_3 adsorption on the brönsted and lewis acid sites of V_2O_5(010): a periodic density functional study. *J. Phys. Chem. B* 103(22):4701-4706.